

TELERAG: Efficient Retrieval-Augmented Generation Inference with Lookahead Retrieval

Chien-Yu Lin*

University of Washington
Seattle, WA, USA
cyulin@cs.washington.edu

Xiaoxiang Shi†

Shanghai Jiao Tong University
Shanghai, China
lambda7shi@sjtu.edu.cn

Rulin Shao

University of Washington
Seattle, WA, USA
rulins@cs.washington.edu

Stephanie Wang

University of Washington
Seattle, WA, USA
smwang@cs.washington.edu

Luis Ceze

University of Washington
Seattle, WA, USA
luisceze@cs.washington.edu

Keisuke Kamahori*

University of Washington
Seattle, WA, USA
kamahori@cs.washington.edu

Madhav Kashyap

University of Washington
Seattle, WA, USA
madhavmk@uw.edu

Zihao Ye

University of Washington
Seattle, WA, USA
zhye@cs.washington.edu

Arvind Krishnamurthy

University of Washington
Seattle, WA, USA
arvind@cs.washington.edu

Yiyu Liu*†

Shanghai Jiao Tong University
Shanghai, China
liu_yiyu@sjtu.edu.cn

Yile Gu

University of Washington
Seattle, WA, USA
ylegu@cs.washington.edu

Kan Zhu

University of Washington
Seattle, WA, USA
kanzhu@cs.washington.edu

Rohan Kadekodi

University of Washington
Seattle, WA, USA
rohankad@cs.washington.edu

Baris Kasikci

University of Washington
Seattle, WA, USA
baris@cs.washington.edu

Keywords: RAG inference, Acceleration, Prefetching.

Abstract

Retrieval-augmented generation (RAG) extends large language models (LLMs) with external data sources to enhance factual correctness and domain coverage. Modern RAG pipelines rely on large datastores, leading to system challenges in latency-sensitive deployments, especially when GPU memory is limited. To address these challenges, we propose TELERAG, an efficient inference system that reduces RAG latency with minimal GPU memory requirements. The core innovation of TELERAG is *lookahead retrieval*, a prefetching mechanism that anticipates required data and transfers it from CPU to GPU in parallel with LLM generation. By leveraging the modularity of RAG pipelines, the inverted file index (IVF) search algorithm and similarities between queries, TELERAG optimally overlaps data movement and computation. Experimental results demonstrate that TELERAG achieves up to a **1.53× average reduction** in end-to-end latency for single-query inference and up to **1.83× average improvement** in throughput for batch-query scenarios compared to state-of-the-art systems. This confirms the practical utility of TELERAG for faster and more memory-efficient deployments of advanced RAG applications.

*Equal contribution.

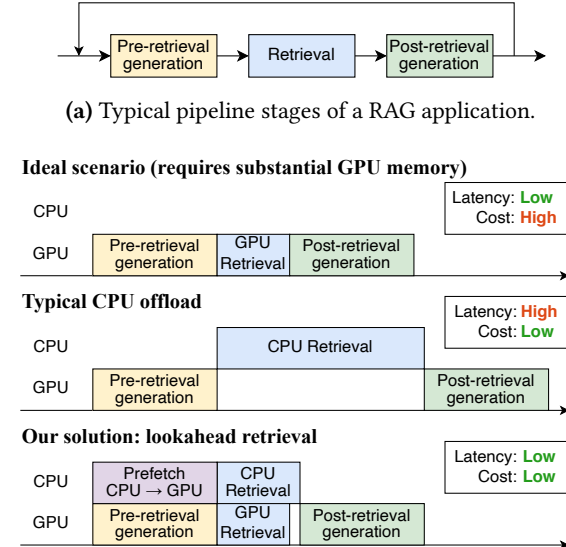
†Work done during internship at University of Washington.

1 Introduction

Retrieval-augmented generation (RAG) has emerged as a powerful technique to enhance large language models (LLMs) by integrating them with external databases [13, 29, 58]. During inference, RAG *retrieves* relevant content from external data sources, usually indexed as vector datastores, to mitigate issues such as hallucinations [51, 64, 76] and incorporate up-to-date or private information [36, 65].

Modern RAG applications share two key characteristics. (1) RAG applications are built as modular pipelines as shown in Figure 1a, where a single query undergoes *multiple rounds* of LLM calls and retrievals, each of which serves different functions to improve overall output quality. For example, query transformation rounds [10, 27, 72, 100] generally occur before retrieval to refine the user’s query with LLMs (pre-retrieval generation). (2) RAG’s *datastores are typically large*, supported by recent works demonstrating that larger datastore consistently improves the performance of RAG applications [16, 33, 51, 65, 79].

These characteristics create several significant challenges for efficient RAG inference, especially in latency-sensitive applications such as customer chatbots [7, 19, 84], financial analysis [63, 66], and emergency medical diagnosis [31, 54].



(b) Illustration of TELERAG’s *lookahead retrieval* mechanism and comparison to different RAG systems. TELERAG prefetches relevant retrieval data from CPU to GPU, overlaps data transfer with the pre-retrieval stage, and accelerates retrieval with GPU-CPU cooperation.

Figure 1. Overview of RAG pipeline stages and comparison of TELERAG to baseline systems.

First, the latency of RAG systems is inherently increased due to multiple rounds of LLM generation and retrieval. Second, although GPUs can speed up both LLM generation and retrieval, the combination of these processes poses significant memory requirements, often exceeding available GPU resources (see §3.1). Hence, it is expensive or even infeasible to fully host both operations on GPUs.

Consequently, in local or custom deployments, which are common for RAG applications with private or sensitive data, the retrieval datastore is often offloaded to CPU memory to alleviate GPU memory constraints. However, while CPU offloading resolves memory limitations, it significantly increases retrieval latency (see §3.1), diminishing overall system efficiency. This memory pressure is not limited to local deployments; even for serving scenarios in data centers, where many concurrent requests are processed together and GPUs are plentiful, managing large index sizes still presents a significant challenge for achieving high throughput with latency service level objectives (SLOs). Allocating additional GPU memory to the retrieval data store directly reduces the memory available for the KV cache of the LLM serving system, limiting the effective batch sizes [56]. In contrast, CPU retrieval would increase the per-request latency by a lot, highlighting the need for techniques that reduce GPU memory consumption while preserving low latency.

To address the latency challenge, several recent works have been proposed to accelerate RAG inference. These approaches include hardware accelerators for retrieval [42, 75],

reuse of KV-cache [45, 61, 93], and speculative document retrieval [87, 99]. However, these works do not address the substantial memory demands associated with retrieval. Therefore, designing a memory-efficient system for low-latency RAG deployments is crucial.

In this paper, we argue that a promising direction to reduce GPU memory usage while maintaining low latency lies in improving the design of the retrieval index. Specifically, the inverted file index (IVF) [81] reduces retrieval latency by pre-clustering data and limiting runtime search to relevant clusters. It offers a way to leverage GPU-accelerated search while not increasing memory consumption by dynamically transferring only the necessary clusters from the CPU to the GPU. However, this data transfer overhead is a key bottleneck, and needs to be minimized [50] (see §3.2).

Our proposal. To tackle latency and memory bottlenecks in RAG inference, we introduce a novel mechanism called **lookahead retrieval**, which predicts the subsets of IVF clusters that will likely be accessed during runtime and proactively transfers them from the CPU to the GPU before the retrieval stage.

The key observation behind lookahead retrieval is that there is substantial semantic overlap between queries *before* and *after* the pre-retrieval stage. Namely, IVF clusters used by the initial input query, which is available well before the retrieval stage, are also likely to be relevant to the actual retrieval query (see §3.3).

Using this insight, we propose TELERAG, an efficient inference system designed to optimize RAG latency while minimizing GPU memory consumption. TELERAG employs lookahead retrieval to preemptively load relevant IVF clusters onto the GPU, effectively hiding CPU-GPU data transfer overhead during concurrent LLM generation. As illustrated in Figure 1b, this approach significantly reduces retrieval latency without exceeding GPU memory constraints, enabling efficient execution of RAG applications. To maintain retrieval accuracy while adopting lookahead retrieval, TELERAG simultaneously searches for clusters that were not prefetched (*i.e.*, mispredicted) from the CPU and merges the results. TELERAG also supports batch and multi-GPU inference.

A key challenge in deploying lookahead retrieval is determining the optimal number of IVF clusters to prefetch: Prefetching too many clusters increases data-transfer overhead, whereas prefetching too few could result in higher retrieval latency due to increased CPU processing. To address this, we propose a profile-guided approach coupled with an analytical model that dynamically determines the ideal prefetch amount based on pipeline characteristics and hardware configurations.

Results summary. We evaluate TELERAG with a popular Wikipedia-based datastore [5] across six popular RAG pipelines built with the Llama model family [83] (3B, 8B, and 13B). Remarkably, TELERAG supports retrieval from a **61 GB datastore** alongside a **Llama3-8B (16 GB)** LLM on a single

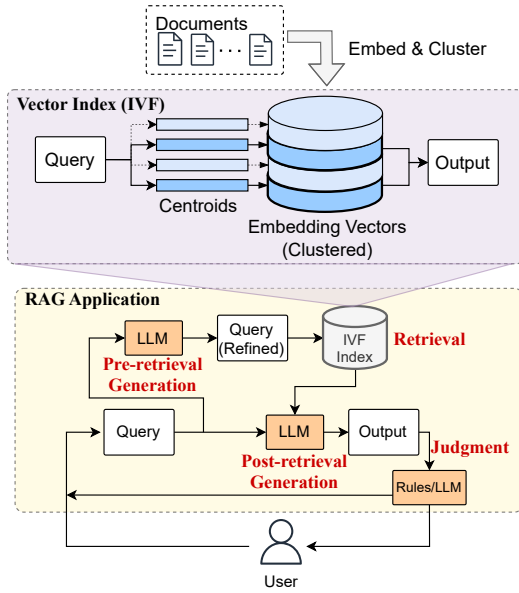


Figure 2. Overview of RAG.

RTX 4090 GPU (**24 GB memory**), significantly outperforming the CPU retrieval baseline. Experiments demonstrate that TELERAG achieves up to a $1.53\times$ average reduction in end-to-end latency for single-query inference on an RTX 4090. In batching scenarios, TELERAG provides even greater throughput enhancements as the batch size increases, achieving $1.83\times$ higher throughput on average at batch size 8 on an H100 GPU. These results underscore TELERAG’s capability to efficiently manage large-scale RAG inference tasks under tight GPU memory constraints, validating its practical benefits for resource-constrained deployments.

In summary, we make the following key contributions:

- Analyzing the correlation of the queries between the pre-retrieval generation and retrieval stages, revealing significant overlap in their corresponding IVF clusters.
- Proposing *lookahead retrieval*, which prefetches likely IVF clusters to the GPU, and hides CPU-GPU data transfer time during pre-retrieval generation.
- Developing TELERAG, an efficient RAG inference system that integrates *lookahead retrieval*, resulting in significant acceleration of RAG with minimal GPU memory usage.

2 Background

2.1 RAG

RAG is a technique that enhances the capabilities of LLMs by integrating them with information retrieval to generate more accurate and relevant text [13, 29, 58]. The core idea behind RAG is to augment the LLM with relevant information retrieved from a large corpus of documents, improving the LLM’s ability to answer questions without hallucinations [51, 64, 76] and generate contents based on up-to-date or private information [36, 65].

RAG workflow. A basic RAG workflow involves several phases, including data store building, retrieval, and interactions with LLMs [23, 24, 28, 34, 71, 85, 89]. In order to build a data store, raw data in various formats is cleaned, converted to plain text, and divided into *chunks*. These chunks are then encoded into vectors using an embedding model and stored in a *vector index*, enabling efficient searching based on similarity. When a user provides a *query*, it is converted into a vector using the same embedding model, and the most similar chunks from the indexed database are retrieved. For a large-scale index, approximate algorithms such as the inverted file index (IVF) [81] (see §2.2 for detail) are commonly used to accelerate the search process. The retrieved chunks, along with the original user query, are combined and given as a prompt to the LLM. The LLM then generates a response that relies on the information provided in the retrieved documents. This approach enables dynamic and informative responses in both single- and multi-turn dialogues [58].

Modularity in modern RAG applications. However, naively integrating document retrieval into LLM generation can cause several issues. For example, the retrieval often struggles to find relevant content and may select irrelevant or mismatched chunks [27, 62, 100], and a single retrieval may not provide sufficient context, necessitating multiple retrieval rounds [29].

To solve these issues, most state-of-the-art RAG models adopt a *modular* approach that employs multiple rounds of LLM calls and retrievals for a single query [23, 26, 28, 29, 34, 89]. Typically, they have the following types of steps (shown in Figure 2):

- *Pre-retrieval generation*, used to assess whether retrieval is needed or to generate queries for retrieval. An example of a *pre-retrieval* technique is query transformation [27, 37, 59, 62, 73, 74, 94, 100, 102], which reformulates the original query to make it clearer and more suitable for the retrieval task.
- *Retrieval*, used to identify relevant documents from the vector data store. This stage takes the output of pre-retrieval generation and generates data for the next stage.
- *Post-retrieval generation*, generates response based on user query and retrieved documents. It can also perform additional process such as summarization [39, 52] or reranking [82, 104] on the retrieved documents.
- *Judgment*, dynamically determines the execution flow. For example, it decides if more iteration is needed to enhance the response. Heuristics or LLMs can be used for judgement stage.

By proceeding through these functions, RAG applications can deliver more precise and contextually appropriate responses, significantly enhancing the capabilities of LLMs for various applications [29, 46].

2.2 Vector Index and Inverted File (IVF)

The *vector index* is a crucial component of RAG applications that retrieves similar items from large datasets of high-dimensional vectors. Given the query vector $x \in \mathbb{R}^D$ and vector database $Y = \{y_0, \dots, y_{N-1}\} \subset \mathbb{R}^D$, which comprises N vectors, the vector index aims to find the k nearest neighbors of x from the database:

$$k\text{-argmin}_{i=0:N} d(x, y_i),$$

where D is the dimensionality of the vector determined by the embedding model, and d denotes the distance function, which is typically the L2-norm or inner product [47].

To improve search efficiency, the inverted file index (IVF) algorithm is widely used for large-scale vector databases due to its simplicity and effectiveness. IVF partitions the data store into *clusters* and restricts searches to the most relevant clusters, reducing the computational cost. To obtain the cluster assignment of each stored vector, it performs clustering algorithm such as k -means [67] and partitions the database into N_c clusters:

$$\{C_1, C_2, \dots, C_{N_c}\} = k\text{-means}(Y, N_c),$$

where C_j is the set of vectors assigned to the j -th cluster, and the cluster centroids $\{c_1, c_2, \dots, c_{N_c}\}$ are obtained by taking the mean of each vectors in $\{C_1, C_2, \dots, C_{N_c}\}$. Then, each database vector $y_i \in Y$ is assigned to the nearest cluster center:

$$\text{Cluster}(y_i) = \text{argmin}_{j=1:N_c} d(y_i, c_j).$$

With the trained centroids and cluster assignment, we can perform a more efficient index search. There are two steps involved in the IVF index searching. First, it will identify the nearest L cluster centroids of a query vector x :

$$\{c_{j_1}, c_{j_2}, \dots, c_{j_L}\} = L\text{-argmin}_{j=1:C} d(x, c_j).$$

This step is also referred to as the coarse-grained search in IVF, as it identifies candidates at the cluster level. Second, the fine-grained search is performed in the L nearest clusters and identify k closest vectors of x :

$$k\text{-argmin}_{y_i \in \cup_{j=1}^L C_{j_i}} d(x, y_i).$$

which involves sorting. In this way, IVF reduces search space and accelerates the retrieval process. Here, the hyperparameter L from the first step is also referred as `nprobe` [25]. When `nprobe` is larger, the IVF retrieval will be more accurate as it search more clusters. However, the retrieve latency is longer as more computation and data are needed.

Since the search process is highly parallelizable among each cluster and each vector, this search algorithm can be highly accelerated by GPUs. Open-source libraries offer efficient GPU implementations [47, 77]. However, IVF does not reduce the memory requirement for the index since the data for all clusters must be stored. As a result, IVF still requires a

substantial GPU memory footprint, which becomes a bottleneck when GPU memory capacity is the constraint of RAG systems. Moreover, recent work reported that increasing the size of the data store positively affects RAG application performance [16, 33, 51, 65, 79], exacerbating this issue.

2.3 Use Cases and Motivation

In this paper, we aim to achieve low-latency RAG inference without driving up GPU memory consumption, which is relevant for both local and data center settings. This goal is critical for efficiently serving a wide range of real-world applications where users expect near-instantaneous responses, thus imposing strict latency SLOs. Examples include customer chatbots [7, 14, 19, 84], financial analysis [63, 66], autonomous driving [18, 95], and emergency medical diagnosis [31, 54].

On the one hand, there is significant demand for RAG applications that involve user-specific private data in local settings [22, 30, 57, 88, 90]. In such scenarios, the available GPU resources are usually limited, and the system serves a single request at a time. Therefore, CPU offloading is necessary when using a large vector index, which introduces substantial latency as we will show in the next section.

On the other hand, for large-scale RAG services in data centers [1, 2, 10], the goal is to serve many concurrent user requests cost-effectively, necessitating high system throughput. However, maximizing LLM serving throughput is often bottlenecked by the GPU memory available for the KV cache, which dictates the maximum possible batch size [56]. If a large retrieval datastore is loaded onto GPUs, it consumes memory that could otherwise be used for a larger KV cache, thereby limiting throughput. Hence, falling back to slow CPU retrieval to save GPU memory is a common option [41], but this is not desirable for latency-sensitive applications due to latency overhead.

In both cases, a straightforward way to reduce inference latency is scaling up GPU resources to allow both the LLM and datastore to reside in GPU memory, which is usually cost-prohibitive. Therefore, in this paper, we aim to design an efficient RAG inference system that can satisfy latency SLOs without requiring a significant amount of GPU memory.

3 Analyzing Latency of RAG Pipelines

In this section, we analyze state-of-the-art RAG applications and identify their underlying systems challenges in achieving low latency. To conduct the analysis, we construct a 61 GB vector index with the Faiss library [25], and set the IVF clusters to 4096 following common practice [11]. We use Llama-3-8B [6] as the LLM, and run our analysis on an RTX 4090 (24 GB memory) and H100 (80 GB memory). §5.2 provides more details about our experimental setups.

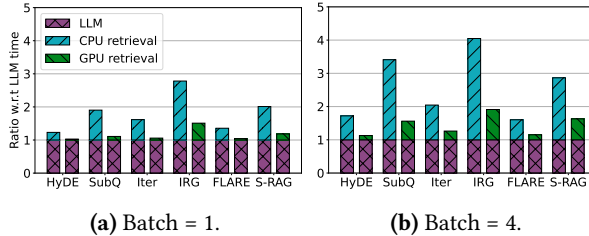


Figure 3. Latency breakdown of six RAG pipelines on NQ dataset [55] with one H100 GPU. nprobe is 256.

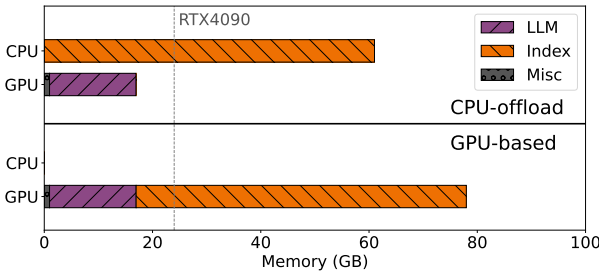


Figure 4. The breakdown of memory consumption at GPU and CPU for two different strategies: CPU offloading and GPU-based retrieval. The dotted line indicates the memory capacity of a RTX4090 GPU, which is a common used GPU for local deployment.

3.1 End-to-end Latency of RAG Pipelines

We first analyze the end-to-end latency of six representative RAG pipelines (see §5.1 for details) in two scenarios: (1) the LLM runs on the GPU, while retrieval is offloaded to the CPU, minimizing GPU memory usage, and (2) both the LLM and the vector index reside in GPU memory, enabling GPU-based retrieval for lower latency. If the GPU’s memory is insufficient, CPU offloading is necessary.

We set the nprobe to 256, a commonly used setting under this index’s configuration (see §5.2 for details), to measure retrieval latency. Figure 3 shows the breakdown of end-to-end latency into LLM inference part and retrieval part, based on 1024 randomly sampled queries from the NQ dataset [55]. We observe that, in the CPU-based retrieval baseline (first scenario), the retrieval phase dominates the latency, consuming 41.1% and 60.5% of total latency for batch sizes 1 and 4, respectively. In contrast, GPU-accelerated retrieval in the second scenario dramatically reduces this bottleneck, accounting for only 10.5% and 28.3% of the latency in comparable configurations. On average, GPU retrieval is 5.96 \times (batch size 1) or 3.87 \times (batch size 4) faster than CPU retrieval, reducing overall latency by approximately 1.5 \times or 1.8 \times , respectively. Thus, accelerating retrieval on the GPU is crucial for improving end-to-end latency.

However, GPU acceleration comes with a significant memory cost. Figure 4 shows the memory requirements for both GPU and CPU. As Figure 4 shows, putting both LLM weights and the retrieval index on the GPU requires around 77 GB of memory, which exceeds the capacity of consumer GPUs

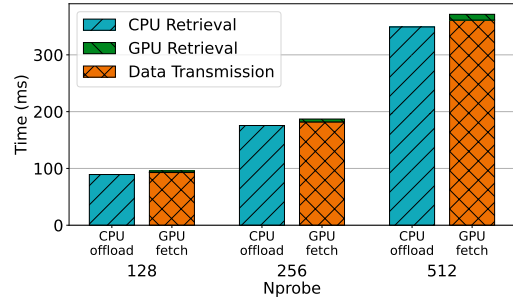


Figure 5. Latency breakdown of CPU-offload and runtime-fetch GPU retrieval, averaged over 512 random NQ queries.

like the RTX 4090 with 24 GB. Thus, GPU acceleration on retrieval is often not feasible when running on a lower-end GPU or indexing with a large datastore.

Even on GPUs capable of holding the entire index in memory (e.g., H100), the index’s memory footprint limits throughput in data center serving scenario. Batched inference maximizes throughput, but it is bottlenecked by the KV cache capacity for LLM serving [56]. For the case of the example above, storing the index on the GPU leaves minimal memory for the KV cache (e.g., ~3 GB, or ~20k tokens worth), restricting batch size, while offloading the index to the CPU significantly increases the available memory (e.g., to >500k tokens worth). This issue is exacerbated since RAG typically involves long contexts [45, 61, 93] and there is a trend of growing model and index sizes [16, 33, 51, 65, 79], increasing memory pressure and necessitating offloading. However, CPU offloading is suboptimal for latency-sensitive applications as discussed above.

Therefore, in the rest of this section, we try to answer the following question: *Is it possible to achieve the latency of GPU-based retrieval while using much less GPU memory?*

3.2 Opportunities of GPU-accelerated Retrieval with Limited Memory

A straightforward approach to enable GPU retrieval with limited GPU memory is to fetch the necessary data from CPU to GPU on-demand for each query, leveraging the IVF index structure that narrows the search space (§2.2). While this method enables faster searching on the GPU, data fetching becomes the bottleneck.

In Figure 5, we compare the latency of the on-demand fetching system against CPU retrieval on an RTX 4090 GPU. We show three different nprobe values that determine the amount of data fetched. Overall, fetch time dominates latency due to the limited PCIe bandwidth between the CPU and GPU (32 GB/s). Although the GPU search is substantially faster than the CPU counterpart, the fetch overhead results in a higher end-to-end latency, which is about 3% slower on average across nprobe values. Thus, to realize any meaningful speedup with this approach, the data fetching latency must be effectively hidden.

Dataset	HyDE [27]	SubQ [59]	Iter [59]	IRG [80]	FLARE [44]	S-RAG [11]
NQ [55]	73.1%	63.2%	91.5%	83.8%	79.1%	100.0%
HotpotQA [92]	75.3%	62.5%	89.6%	89.4%	80.2%	100.0%
TriviaQA [48]	73.1%	61.6%	86.2%	86.1%	81.7%	100.0%

Table 1. IVF cluster overlapping rate between the input and output of the pre-retrieval generation. The nprobe is set to 512. Since Self-RAG does not incorporate query transform, its coverage is always 100%.

To hide data fetch costs, CPU-to-GPU transfer must precede retrieval, which requires predicting which data will be accessed. Fortunately, as we show next, the modern RAG pipelines offer a valuable hint as a query at the previous step.

3.3 Overlapping of IVF Clusters

While the exact data to be retrieved is only known after the pre-retrieval generation is done, we observe that there are high similarities of the IVF clusters assignments between the queries at different stages.

Similarity of queries at different stages. During the pre-retrieval process of RAG pipelines (e.g., query transformation [27, 37, 59, 62, 73, 74, 94, 100, 102]), an LLM call is issued to refine an initial user query q_{in} into a transformed query q_{out} , which is then used for retrieval. This process often rewrites the query into a different format [27] or simplifies its complexities [59], which intuitively preserves the query’s core semantic content. Hence, the embedding vectors of q_{in} and q_{out} are likely to be similar. This similarity, in turn, suggests that the IVF clusters to which these queries would be assigned will overlap. Therefore, q_{in} can serve as a valuable hint for predicting subsequent memory accesses.

Prediction coverage. To verify this hypothesis, we evaluate the average cluster coverage rate between prefetched clusters and clusters used for retrieval in three popular question-answer datasets (NQ [55], HotpotQA [92], and TriviaQA [48]) and six RAG pipelines. Table 1 shows the coverage when we prefetch 256 clusters. From the table, we observe that IVF cluster overlap rates are consistently high across a range of datasets and pipelines. For instance, even the lowest reported values remain above 61.6% (for SubQ).

Opportunity. This data shows an opportunity for predicting required clusters, which can make it possible to hide data transfer overhead during LLM generation. In this paper, we aim to leverage this observation to accelerate the inference latency for RAG.

4 Design of TELE-RAG

Based on the high IVF cluster overlapping observation presented in §3.3, we propose TELE-RAG, an efficient RAG inference system that utilizes lookahead retrieval to prefetch a minimal set of likely IVF clusters to GPU, and accelerate the retrieval process. In this section, we detail the design of lookahead retrieval and implementation of TELE-RAG.

4.1 Overview

Figure 6 presents the overview of TELE-RAG with lookahead retrieval. In Figure 6, q_{in} denotes the initial input to the pre-retrieval stage and q_{out} denotes its output, *i.e.*, the query given to the subsequent retrieval stage. We highlight the IVF clusters corresponding to q_{in} and q_{out} with a red background (C_{in}), and a blue background (C_{out}), respectively. Due to the semantic similarity of q_{in} and q_{out} , there is significant overlap between C_{in} and C_{out} , marked with a purple background ($C_{overlap}$).

Given this, the proposed lookahead retrieval technique in TELE-RAG operates in three key steps:

- Pre-retrieval & data transfer:** During LLM generation, identify C_{in} and transfer corresponding data to GPU memory, prioritizing clusters closest to q_{in} . This leverages GPU DMA for concurrent transfer of clusters data and compute of LLM generation.
- GPU similarity search:** After identifying C_{out} , the GPU efficiently performs a similarity search on the predicted clusters ($C_{overlap}$) already in its memory.
- CPU similarity search:** Concurrently with the GPU search, the CPU processes the similarity search for the missed clusters (C_{miss}) that were not prefetched to the GPU, reducing the CPU’s overall workload.

In summary, our lookahead retrieval speeds up retrieval by overlapping data prefetching to the GPU with LLM generation and performing concurrent similarity searches on both the GPU (for predicted clusters) and CPU (for the remainder), significantly reducing the CPU’s computational workload.

4.2 Finding the Optimal Prefetch Amount

A key challenge in TELE-RAG is to balance the benefit of reducing retrieval latency by prefetching data against the overhead of CPU-GPU transfers. Prefetching more clusters reduces the subsequent retrieval time but can also extend the transfer phase; if it extends beyond the LLM generation window, we lose the advantage of overlap and potentially introduce additional delay. Still, additional delays in data transfer may be worthwhile if they substantially reduce retrieval latency. To guide the choice of the optimal amount of data to prefetch, we develop a mathematical model based on profile information.

Mathematical model. Here, we denote b_p as the number of bytes to prefetch and B as the CPU-GPU bandwidth. The optimal amount of data to prefetch is denoted as b_p^* . To start, we let t_1 represent the combined time of prefetching and pre-retrieval LLM generation, and t_2 represents the retrieval time. We have: $t_1 = \max(t_{LLM}, t_p)$ and $t_2 = \max(t_c, t_g)$, where t_{LLM} is the time for LLM generation, t_p is prefetching time, t_c is the CPU retrieval time, and t_g is the GPU retrieval time. The objective is to minimize $t_1 + t_2$.

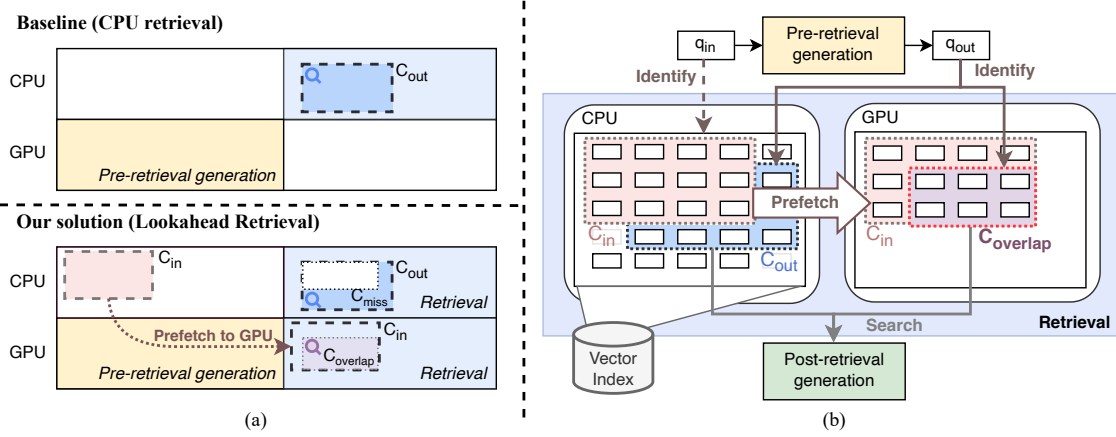


Figure 6. (a) The overview of **lookahead retrieval** compared against CPU-offloaded retrieval, and (b) the system design of TELERAG. After identifying clusters (C_{in}) for the initial query q_{in} , C_{in} is transferred to the GPU while concurrently generating q_{out} . At retrieval time, the GPU searches prefetched clusters while the CPU handles remaining ones, before results are merged.

Since prefetching time t_p is proportional to b_p , we express t_1 as a piecewise function:

$$t_1 = \begin{cases} t_{LLM}, & \text{if } b_p \leq B \cdot t_{LLM}, \\ \frac{b_p}{B}, & \text{if } b_p > B \cdot t_{LLM}, \end{cases} \quad (1)$$

From Eq. 1, if we prefetch fewer bytes than can be transferred during LLM generation, t_1 is effectively just t_{LLM} because the transfer overlaps completely with LLM execution.

As shown in §3.1, GPU retrieval (t_g) is generally much faster than CPU retrieval (t_c). Thus, we assume $t_c \gg t_g$. As CPU has a limited parallelism, t_c usually grows proportionally with the number of clusters to be processed [40]:

$$t_2 = t_c = r_{\text{miss}} \times n_{\text{probe}} \times t_{cc}, \quad (2)$$

where r_{miss} is the miss rate (percentage of IVF clusters are not caught on GPU), n_{probe} is the total number of clusters to search, and t_{cc} is the CPU time to search a single cluster. Increasing b_p can only decrease or maintain the current miss rate, i.e., $\frac{dr_{\text{miss}}}{db_p} \leq 0$. Moreover, because clusters are prefetched in order of descending likelihood, we assume r_{miss} is either linear or a concave up function¹ of b_p , i.e., $\frac{d^2r_{\text{miss}}}{db_p^2} \geq 0$.

We now examine two cases:

- **Case 1:** $b_p^* \leq B \cdot t_{LLM}$. Here, $t_1 = t_{LLM}$ is constant because prefetching is fully overlapped with LLM generation. Since increasing b_p in this regime will not increase t_1 and cannot worsen the miss rate, pushing b_p to the boundary $B \cdot t_{LLM}$ minimizes $t_1 + t_2$. Hence,

$$b_p^* = B \cdot t_{LLM}. \quad (3)$$

- **Case 2:** $b_p^* > B \cdot t_{LLM}$. In this region, t_1 grows linearly with b_p , and we have: $\frac{d^2}{db_p^2} (t_1 + t_2) = \frac{d^2r_{\text{miss}}}{db_p^2} \cdot n_{\text{probe}} \cdot t_{cc} \geq$

0. Therefore, $t_1 + t_2$ is concave up, allowing at most one minimum. At the minimum point, we have:

$$\frac{d}{db_p} (t_1 + t_2) = 0 \implies \frac{1}{B} + \frac{dr_{\text{miss}}}{db_p} \cdot n_{\text{probe}} \cdot t_{cc} = 0. \quad (4)$$

From this, we obtain:

$$b_p^* = B \times n_{\text{probe}} \times t_{cc} \times \Delta r_{\text{miss}}, \quad (5)$$

where Δr_{miss} is the decrement of the miss rate for this round. If b_p^* is indeed larger than $B \cdot t_{LLM}$, it becomes the global minimum; otherwise, the solution reverts to Case 1.

In summary, our analysis shows that the optimal prefetch amount b_p^* can only lie at one of two points: (1) Prefetch until LLM generation completes (i.e. $b_p = B \cdot t_{LLM}$). (2) A point determined by Eq. 5. However, under typical CPU-GPU bandwidth (e.g., 55 GB/s on PCIe 5), the time spent loading additional clusters often outweighs any retrieval latency reduction from lowering r_{miss} . Consequently, the second scenario in Eq. 5 becomes nearly infeasible in practice. Therefore, on current hardware, *prefetching exactly until LLM execution ends* is generally the most effective choice.

Profiling-guided approach. Although b_p^* can be derived from the analysis above, it depends on knowing t_{LLM} for each query, which cannot be obtained ahead of time. To address this, we use a *profiling-guided approach*, leveraging the observation that, despite differences in query content, the output length (and thus generation time) for a RAG pipeline often remains similar across most queries. Accordingly, for each RAG pipeline, we can measure t_{LLM} on a calibration set containing n queries, and get estimated $\hat{b}_p^* = B \cdot \bar{t}_{LLM}$, where $\bar{t}_{LLM} = \text{mean}\{t_{LLM,1}, t_{LLM,2}, \dots, t_{LLM,n}\}$. This estimated \hat{b}_p^* can then be used for incoming queries, ensuring a near-optimal prefetch amount.

¹An upward U-shaped function whose second derivative is positive.

4.3 Design Details

Sorting Optimization. TELERAG accelerates the final k -argmin sorting step of IVF search by leveraging GPU. Because each cluster may contain thousands of points, sorting is particularly well-suited to GPU parallelism [9]. To enable this, TELERAG transfers the scalar distance values computed on the CPU for C_{miss} to the GPU. Unlike full vector data, this transfer incurs negligible overhead. The GPU then performs a global sort over the combined distances from C_{overlap} and C_{miss} , delivering end-to-end speedups than the CPU-only retrieval systems.

Prefetch Target. TELERAG’s prefetching mechanism targets a specific number of bytes (b_p) rather than the number of clusters to ensure more predictable performance. Since IVF cluster sizes are often highly uneven, targeting a fixed cluster count can lead to unstable data loading times, whereas a byte limit provides a clearer upper bound on the transfer duration based on bandwidth.

When selecting clusters to meet the prefetch byte budget (b_p), the system adds whole clusters sequentially based on proximity to the query. If adding the next closest cluster would exceed the budget, it is omitted entirely rather than being partially loaded, ensuring a clean division where each cluster is processed exclusively by either GPU or CPU.

Multi-Round Support. For multi-round RAG involving the same input query, the system performs a full prefetch (up to the budget) only in the first round, leveraging high cluster similarity across rounds. In subsequent rounds, it incrementally fetches only the additional required clusters that were not loaded previously, optimizing data transfer while respecting the memory budget.

Batch Support. For batch inference, a challenge for lookahead retrieval is that each query requires a different set of IVF clusters. In our design, we fix the prefetching budget to the amount we got from §4.2 irrespective of batch size, and equally distribute the budget to each query in a batch. As a result, although the average cluster hit rate per request will decrease for larger batch sizes, we can ensure each query’s retrieval search time is equally accelerated, forming a balanced batched retrieval.

Multi-GPU support. For multi-GPU systems, we perform a greedy search based on embedding similarities of queries to group similar queries into mini-batches, and distribute the mini-batches among GPUs. The greedy search is efficient and incurs negligible overhead: In our profiling for up to the batch size of 256, the latency to perform greedy search is less than 0.1 s, which is minimal compared to the end-to-end latency of each batch.

4.4 Implementation Details

TELERAG is implemented in Python and also leverages PyTorch’s [8] operator ecosystem for efficient computation. The datastore index is initially constructed using FAISS [25],

Specification	Value
Dataset	wiki_dpr [49]
Dataset size	2.1 billion tokens
# of chunks	21 million
# of IVF cluster	4096
Embed model	Contriever [35]
Embed dimension	768
Index type	FLAT ²
Distance metric	Inner Product
Index size	61 GB

Table 2. Detailed configurations of our retrieval index.

and its data structures, such as IVF centroids and cluster data, are converted to PyTorch tensors.

At runtime, cluster data is loaded into a contiguous pinned memory region on the CPU, enabling non-blocking memory copies to the GPU. A fixed-size contiguous buffer on the GPU is allocated based on the user’s configuration or GPU memory capacity during runtime.

To enable concurrent CPU-GPU data transferring and LLM generation, we utilize the `_copy(non_blocking=True)` API in PyTorch and use separate CUDA streams for prefetching and LLM. In this way, the data copy operations will not block the GPU to perform computation, and thus the TELERAG can do prefetching in parallel to the pre-retrieval LLM generation.

To implement the index search with GPU-CPU cooperation, for the GPU part, we use a single matrix-vector multiplication that computes distances for all prefetched vectors; for the CPU part, we utilize multithreading in Python to parallelize similarity searches across clusters. We then move the distances computed from CPU to GPU, merge with distances on GPU and perform global sorting on GPU.

5 Evaluation

We conduct extensive experiments to evaluate the effectiveness of TELERAG. In this section, we describe the necessary details on how we set up the evaluations, present experimental results, and provide in-depth analysis and discussions.

5.1 Evaluation Datasets and RAG Models

Datastore. We build a datastore based on the wiki_dpr dataset [49], a popular dataset that contains 2.1 billion tokens from Wikipedia. Following previous works [11, 49, 65], we chunk the passages by every 100 tokens, and use Contriever [35] to generate an embedding for each chunk. The embeddings have a hidden dimension of 768.

Vector index. For the baseline retrieval, we build an IVF vector index using Faiss [25] on the datastore. As described in §4.4, we convert the Faiss index to a customized index in PyTorch for TELERAG. See Table 2 for the detailed configurations of our vector index and datastore.

²Original embedding without compression for the best retrieval precision.

Setup	Desktop	Server
CPU	Threadripper 5975	EPYC 9554
CPU memory size	512 GB	1.5 TB
GPU	RTX4090 [68]	H100 [69]
GPU memory size	24 GB	80 GB
CPU-GPU Bus Bandwidth	PCIe 4 32 (24) GB/s	PCIe 5 64 (51) GB/s

Table 3. Hardware specifications for our setups. In bandwidth, the number in the parentheses is the actual bandwidth we measured from our system.

LLMs. We evaluate TELERAG on the Llama model family [83] in three different sizes (Llama-3.2-3B, Llama-3-8B, Llama-2-13B) to represent different use cases.

RAG pipelines. We evaluate TELERAG with six popular RAG pipelines. Figure 7 shows the overview of each pipeline. Note that although some pipelines lack pre-retrieval generation, the post-retrieval generation serves similar functionality for the retrieval of the next iteration. Below are brief descriptions of the evaluated RAG pipelines.

1. **HyDE** [27] prompts LLM to generate a hypothetical paragraph and perform retrieval based on the embedding of the generated paragraph.
2. **SubQuestion (SubQ)³** [59] prompts LLM to generate multiple sub-questions and performs retrievals for each generated sub-question.
3. **Iterative (Iter)⁴** [59] prompts LLM to generate narrower questions first and iteratively refine them based on previous answers. At the end of each iteration, it prompts LLM to judge if the answer is good enough.
4. **Iter-RetGen (IRG)** [80] iteratively do retrieval and LLM generation for 3 iterations.
5. **FLARE** [44] iteratively issues retrievals based on the confidence (probability score) of predicted tokens for the upcoming sentence.
6. **Self-RAG (S-RAG)⁵** [11] uses the LLM to judge for retrieval, generate responses, and self-critique on the responses. We use fine-tuned models based on Llama2-7B and Llama2-13B from their official repository [12].

Evaluation Datasets. We use three commonly used question-answering datasets, NQ [55], HotpotQA [92], and TriviaQA [48]. For each dataset, we randomly sample 1024 queries and report the average unless otherwise specified.

5.2 Experiment Setups

Hardware setups. We evaluate TELERAG on two hardware environments, Desktop and Server, which are equipped to represent the settings for the desktop and data center use cases. The Desktop has the RTX4090 (24 GB memory), and we use 3B and 8B models. The Server has the H100 (80 GB memory), and we use 8B and 13B models. These sizes

³Implemented in LlamaIndex as SubQuestionQueryEngine.

⁴Implemented in LlamaIndex as MultiStepQueryEngine.

⁵We evaluate on the short-form version which only has one iteration.

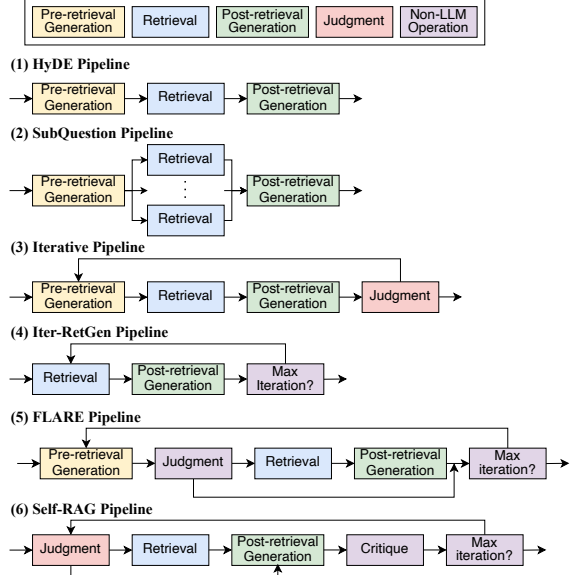


Figure 7. Overview of six RAG pipelines that we evaluate.

represent common model sizes for RAG applications [10, 11]. We do not evaluate the 13B model on Desktop as its model size (26 GB) exceeds RTX4090’s memory capacity. Table 3 summarizes the hardware configurations.

Nprobe and top- k . For the IVF index, nprobe is a hyperparameter that controls the trade-off between search efficiency and retrieval quality. A common heuristic is to set nprobe to $4\sqrt{N_c}$ [105]. Given our index size of $N_c = 4096$, we use nprobe = 256 ($= 4\sqrt{4096}$) by default, unless otherwise specified. For retrieval, top- k denotes the number of most relevant documents to return. We use top- k = 3, which is a standard choice in RAG.

RAG pipeline implementation. We implement the RAG pipelines with the FlashRAG framework [46]. For IRG, FLARE, and S-RAG, we use the framework’s default implementations. For the other pipelines, we reimplement them using FlashRAG’s APIs.

Benchmark methodology. We follow a benchmarking methodology from SGLang [101] and use GPT-3.5-Turbo [70] to run through each pipeline and record the input and output text of each step. During latency evaluation, we set the LLM’s output length based on the recorded text. This way, we ensure a fair latency comparison across different LLM models.

Baseline systems. To evaluate the latency of each pipeline, we construct a clean execution flow in Python that only contains LLM generation, datastore retrieval, and other necessary logical operations to fulfill each pipeline. For LLM generation, we use SGLang [101], which is a state-of-the-art LLM inference engine. For retrieval, we use a popular retrieval library, Faiss [25], as the CPU-offloaded baseline.⁶

⁶This baseline resembles frameworks like LlamaIndex and LangChain, which primarily function as wrappers around LLM serving and retrieval

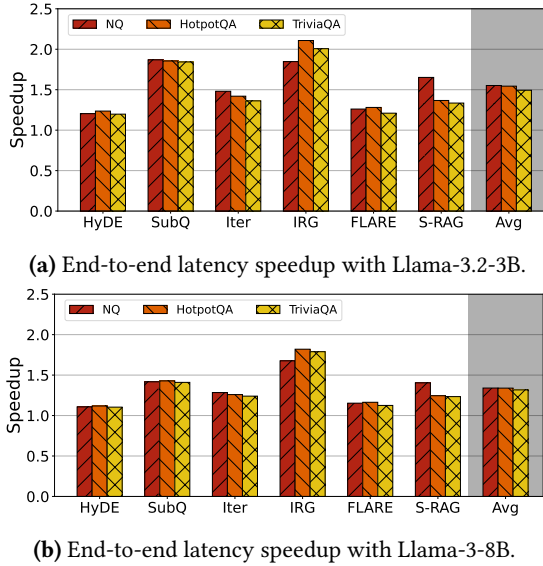


Figure 8. End-to-end latency speedup of TELERAG and baseline on six RAG pipelines and three datasets, with RTX4090 GPU. nprobe is 256.

Prefetching budget setups. Based on the methodology we described in §4.2, we profile each RAG pipeline with a small amount of 64 random samples from NQ [55] and derive the prefetching budget of each pipeline.

Max prefetching memory. We set a maximum GPU memory limit for prefetching in each configuration. For Server, we allocate up to 16 GB. For Desktop, we allocate up to 10 GB and 3.75 GB for the 3B and 8B models, respectively. These settings demonstrate that TELERAG can efficiently operate using only a small fraction (up to 40% for RTX4090 and 20% for H100) of total GPU memory.

5.3 Evaluation Results

Single-query latency on RTX4090. We evaluate the end-to-end RAG latency for single queries on Desktop equipped with RTX4090, representing a typical local scenario. Figure 8 shows the latency reduction of TELERAG across three datasets and two LLMs (Llama-3.2-3B and Llama-3-8B).

As shown in Figure 8, TELERAG consistently outperforms the baseline across all tested configurations. With Llama-3.2-3B, TELERAG achieves average speedups of 1.55 \times , 1.54 \times , and 1.49 \times on NQ, HotpotQA, and TriviaQA, respectively. The best speedup of 2.11 \times is achieved in the Iter-RetGen pipeline on HotpotQA, because this pipeline involves frequent retrieval operations and generally short LLM outputs, which enhances the relative impact of retrieval acceleration.

Another notable improvement is in the SubQuestion pipeline, where TELERAG achieves approximately 1.85 \times speedup

libraries. We build a system from the ground up to avoid the overhead introduced by their complex layers designed for advanced functionality.

across all datasets. This pipeline uses LLM-generated sub-questions and performs batched retrievals of 3 to 4 queries simultaneously. CPU-based retrieval suffers from limited parallelism in such scenarios, but TELERAG efficiently utilizes GPU parallelism, significantly enhancing performance.

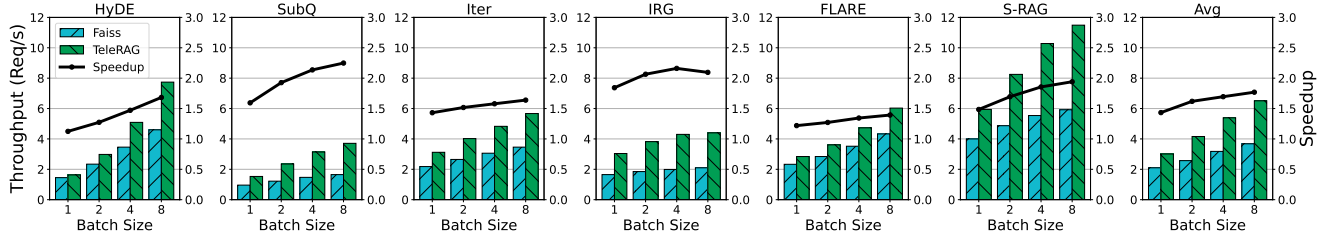
When deploying Llama-3-8B, speedups with TELERAG slightly decrease compared to Llama-3.2-3B, primarily due to increased LLM latency and reduced available memory for prefetching. Still, TELERAG achieves approximately 1.3 \times speedup across datasets, with a peak improvement of 1.82 \times for Iter-RetGen pipeline on HotpotQA. Achieving these results with only 3.75 GB of remaining GPU memory (after accounting for Llama-3-8B (16 GB), the embedding model (1 GB), and other miscellaneous tensors) highlights TELERAG’s robust capability in accelerating RAG inference even under tight GPU memory constraints.

Multi-query throughput on H100. To evaluate the TELERAG’s performance in batched inference, we evaluate the end-to-end throughput on Server (H100) in batch sizes 1, 2, 4, and 8. We show the results of six evaluated RAG pipelines with Llama-3-8B and Llama-2-13B in Figure 9.

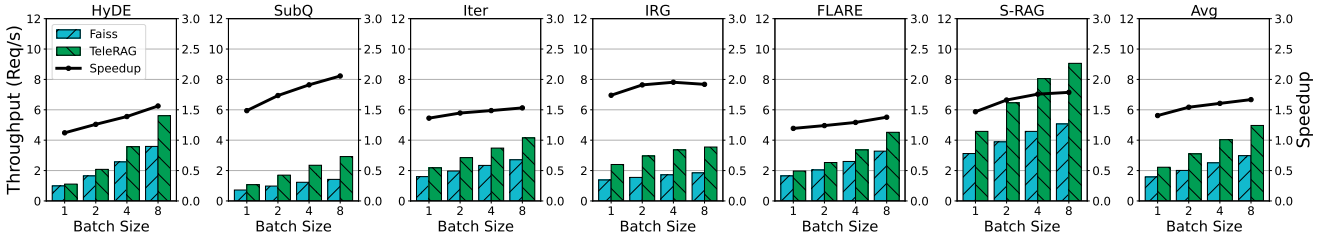
As shown in Figure 9, TELERAG consistently outperforms the Faiss baseline across all pipelines and batch sizes in both LLM sizes. At batch size 1 and running with Llama-3-8B (equivalent to the single-query setting), TELERAG delivers a throughput increase of 1.1 \times to 2.2 \times , with an average of 1.46 \times . As the batch size increases, the performance gains of TELERAG continually grow. The Faiss baseline demonstrates near-linear scalability up to a batch size of 4, but reaches a noticeable plateau at a batch size of 8, indicating that the CPU baseline’s capacity to handle a high volume of simultaneous queries is limited. In contrast, TELERAG continues to scale nearly linearly through the largest batch evaluated, reaching 1.4–2.2 \times higher throughput and an average throughput increase of 1.83 \times at batch 8. The biggest throughput gain is achieved for SubQuestion, up to 2.2 \times at batch 8. This is again due to their higher demands on the retrieval, leaving higher optimization space for TELERAG.

Multi-GPU Throughput. We also evaluate TELERAG in a multi-GPU system to further show the scalability. For the evaluation, we construct a simulation framework around our single-GPU implementation. We first define a global batch size that the whole system will process at once, and then we construct mini-batches to distribute among each GPU. To form a mini-batch, we perform a greedy search based on the embedding similarity of queries, grouping similar queries into the same mini-batch to maximize the cluster hit rate. We present the simulated throughput of TELERAG with a global batch size of 128 and mini-batch size of 4 with 1 to 8 GPUs. As shown in Figure 10, TELERAG’s throughput scales well with the number of GPUs. When compared to 1 GPU

⁷Results for 1 GPU are real, not simulated.



(a) End-to-end throughput with six pipelines and different batch sizes using Llama-3-8B.



(b) End-to-end throughput with six pipelines and different batch sizes using Llama-2-13B.

Figure 9. End-to-end throughput of TELERAG and the baseline across six RAG pipelines on the NQ dataset using Llama-3-8B and Llama-2-13B at different batch sizes on a H100 GPU. The nprobe is set to 256, and the x -axis represents the batch size.

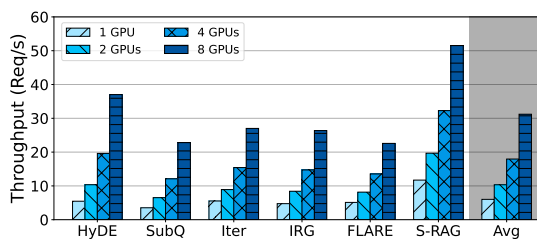


Figure 10. Simulated throughput⁷ of TELERAG on NQ dataset with different number of H100 GPUs.

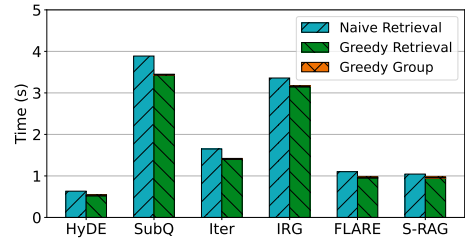


Figure 12. Comparison of end-to-end retrieval latency for two batching strategies: naive mini-batching and similarity-aware greedy grouping. The Greedy Group bars are too short to be visible.

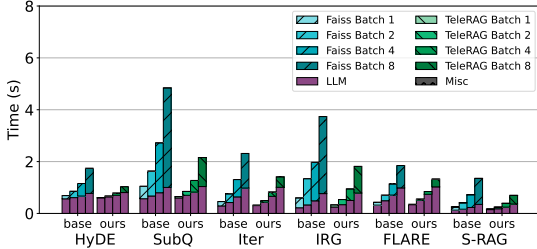


Figure 11. Latency breakdown for Llama-3-8B on NQ with a H100 GPU in different batch sizes. nprobe is 256.

results, the averaged throughput enhancements of TELERAG are $1.7\times$, $3.1\times$, and $5.4\times$ with 2, 4, and 8 GPUs, respectively.

5.4 Analysis and Sensitivity Study

Latency breakdown. We further show the latency breakdown of running RAG pipelines with Llama-3-8B and Llama-2-13B on a single H100 GPU in different batch sizes in Figure 11. From Figure 11, we can observe that LLM latency grows sub-linearly with larger batch sizes. However, the

latency for Faiss retrieval on CPU grows linearly with the batch size, dominating the overall latency when batch size is large. These results echo our findings in Figure 9, and show limited scalability of CPU retrieval in serving scenario. In contrast, TELERAG significantly accelerates across all batch sizes and achieves a higher speedup from $1.4\times$ to $1.8\times$ when the batch size increases from 1 to 8.

Ablation on mini-batch strategies. In our multi-GPU results, we implement a greedy grouping strategy for mini-batching based on queries' similarity in a global batch. Here, we examine the benefits and overhead of this strategy in Figure 12, where we show the end-to-end retrieval latency for mini-batch size 4 with four GPUs and a global batch of 128 queries. The grouping overhead is minimal and the overall retrieval latency of greedy grouping mini-batching consistently outperform naive mini-batching across all pipelines.

Retrieval speedups across nprobe. Figure 13 shows the retrieval latency reduction on NQ. We observe consistent speedups for all nprobe values. The greatest speedups are achieved at nprobe 256, with average speedups of $7.21\times$ and

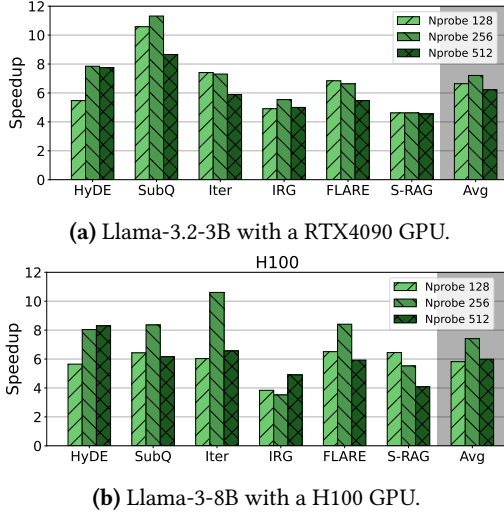


Figure 13. Single-query retrieval speedup on NQ with different nprobe values.

Pipeline	H100 (Llm3-8B)		4090 (Llm3-3B)	
	Budget	Hit Rate	Budget	Hit Rate
HyDE	9 GB	91.95%	7 GB	87.42%
SubQ	8 GB	79.04%	7 GB	76.38%
Iter	5 GB	95.51%	3 GB	84.59%
IRG	4 GB	59.52%	2.5 GB	50.34%
FLARE	6 GB	79.35%	3 GB	56.67%
S-RAG	3 GB	71.29%	1.25 GB	29.96%

Below the table is a horizontal bar chart showing the prefetch budget distribution. The x-axis is labeled from 0% to 100% in 20% increments. The bar is divided into segments: 0% to ~40% is light green, ~40% to ~60% is medium green, and ~60% to 100% is dark green. A legend below the bar shows the same color-coding for the budget levels.

Table 4. The prefetch budget and corresponding averaged cluster hit rate for each pipeline and hardware setup on NQ dataset. The target retrieval nprobe is 256.

7.41× on RTX4090 and H100, respectively. As a larger nprobe value is used, the retrieval performance of TELERAG becomes constrained by missed clusters on the CPU, given our fixed prefetch budget across varying nprobe values. However, RAG inference with higher nprobe will result in longer latency spent on the retrieval and hence, TELERAG still has a significant latency improvement against the CPU retrieval baseline.

Prefetch budgets and cluster hit rates. Table 4 shows the prefetch budgets we set with the profile-guided approach on RTX4090 and H100 for NQ. It also presents the average cluster hit rate achieved with this prefetch budget. From the table, we can see that it generally achieves a high cluster hit rate (>50%) when TELERAG has a large prefetching budget. For cases where the budget is less than 2 GB, we observe a relatively lower hit rate (<50%), limiting the benefits of reducing the CPU’s search workloads. However, as observed from Figure 8, TELERAG achieves from 1.2× to 1.6× end-to-end speedups for these pipelines, thanks to the combined benefit of reducing CPU workload and utilizing the GPU to perform sorting on similarity distances.

6 Related Work

6.1 Systems for RAG

RAGCache [45] proposes a caching system that stores KV caches from datastore chunks in an order-aware manner to improve the time to the first token. This approach only reduces prefetch latency, leaving retrieval and decode times unaffected, despite the fact they typically dominate total latency [4]. Moreover, it assumes repeated use of the same document across multiple requests, limiting its scalability over large data stores. Similarly, TurboRAG [61] precomputes KV caches from the data store, but it also only optimizes prefetch latency. CacheBlend introduces a selective KV-cache fusion technique for RAG to reuse pre-computed caches [93].

RaLMSpec [99] proposes speculative retrieval and batched verification, Chameleon [42] proposes a CPU-GPU-FPGA heterogeneous architecture for accelerating the retrieval process, and PipeRAG [43] is an algorithm-system co-design technique to overlap the retrieval and generation by modifying the algorithms. However, these works focus on the paradigm of RAG that retrieves documents once every few tokens and do not apply to modular RAG applications that are widely used now, as discussed in §2.1.

Speculative RAG [87] introduces drafting by smaller LLMs to reduce RAG latency, but it does not target the retrieval latency. APIServe (InferCept) [3] proposes a novel KV cache management strategy that can support the interception of LLM generation by other workloads, including retrieval. However, this work again does not focus on optimizing retrieval latency. EdgeRAG [78] reduces the memory requirement of retrieval by re-generating and caching document embeddings at runtime, targeting extremely resource-constrained environments. RAGO [41] introduces an abstraction for RAG to automatically pick task placement, resource allocation, and batching policies.

Unlike all these prior works, we tackle system challenges of long retrieval latency and large memory requirement for modular RAG pipelines with large-scale datastores.

6.2 Systems for Compound LLM Applications

Apart from RAG, there is a growing interest in compound or agentic LLM applications, where multiple LLM calls and other applications are combined to serve complex functionalities [15, 86, 96]. LLMCompiler [53] is a framework that optimizes the execution of multiple functions in large language models by enabling parallel function calling. AI Metropolis [91] accelerates LLM-based multi-agent simulations with out-of-order execution. RAG is a specific type of application in this broader direction, and we propose systems techniques to optimize its execution latency, focusing on the characteristics of retrieval workload.

6.3 Vector Index

Vector index is a key component of RAG [17, 29], and many works have been proposed to improve their efficiency. ScaNN proposes an anisotropic quantization method for better efficiency [32]. DiskANN and SPANN propose memory-disk hybrid indexing systems that work beyond the limitation of memory capacity [20, 38]. Other prior works propose hardware acceleration of vector index with GPUs [47], FPGAs [40, 97], TPU [21], or ray tracing hardware [60, 103]. BANG proposes a method to scale graph-based ANN beyond GPU memory [50], and Rummy allows the index to scale beyond GPU memory capacity with reordered pipelining [98]. These methods either require algorithm modifications or are bottlenecked by CPU-GPU bandwidth. Our proposal, focuses on the context of modular RAG applications, where queries for retrieval are usually generated by LLMs, and optimizes the latency and the GPU memory consumption without altering the algorithm of the IVF index.

7 Conclusion

In this paper, we introduced TELERAG, an inference system that tackles the system challenges of RAG pipelines under latency-sensitive scenarios. By using lookahead retrieval, which overlaps data transfer and GPU computation for faster retrieval, a profile-guided approach to determine optimal prefetching data amount, and GPU-CPU cooperation, TELERAG speeds up the end-to-end latency with minimal GPU memory requirement. Our evaluation shows that TELERAG significantly improves performance compared to existing state-of-the-art solutions.

References

- [1] [n. d.]. Genspark. <https://www.genspark.ai/>.
- [2] [n. d.]. Perplexity. <https://www.perplexity.ai/>.
- [3] Reyna Abhyankar, Zijian He, Vikranth Srivatsa, Hao Zhang, and Yiyi Zhang. 2024. APIServe: Efficient API Support for Large-Language Model Inferencing. *arXiv preprint arXiv:2402.01869* (2024).
- [4] Amey Agrawal, Nitin Kedia, Ashish Panwar, Jayashree Mohan, Nipun Kwatra, Bhargav S Gulavani, Alexey Tumanov, and Ramachandran Ramjee. 2024. Taming Throughput-Latency Tradeoff in LLM Inference with Sarathi-Serve. *arXiv preprint arXiv:2403.02310* (2024).
- [5] AI@Meta. 2020. Dataset Card for “wiki_dp”. https://huggingface.co/datasets/facebook/wiki_dpr.
- [6] AI@Meta. 2024. Llama 3 Model Card. https://github.com/meta-llama/llama3/blob/main/MODEL_CARD.md.
- [7] Rama Akkiraju, Anbang Xu, Deepak Bora, Tan Yu, Lu An, Vishal Seth, Aaditya Shukla, Pritam Gundecha, Hridhay Mehta, Ashwin Jha, et al. 2024. FACTS About Building Retrieval Augmented Generation-based Chatbots. *arXiv preprint arXiv:2407.07858* (2024).
- [8] Jason Ansel, Edward Yang, Horace He, Natalia Gimelshein, Animesh Jain, Michael Voznesensky, Bin Bao, Peter Bell, David Berard, Evgeni Burovski, Geeta Chauhan, Anjali Choudria, Will Constable, Alban Desmaison, Zachary DeVito, Elias Ellison, Will Feng, Jiong Gong, Michael Gschwind, Brian Hirsh, Sherlock Huang, Kshitij Kalambarkar, Laurent Kirsch, Michael Lazos, Mario Lezcano, Yanbo Liang, Jason Liang, Yinghai Lu, C. K. Luk, Bert Maher, Yunjie Pan, Christian Puhrsch, Matthias Reso, Mark Saroufim, Marcos Yukio Siraichi, Helen Suk, Shunting Zhang, Michael Suo, Phil Tillet, Xu Zhao, Eikan Wang, Keren Zhou, Richard Zou, Xiaodong Wang, Ajit Mathews, William Wen, Gregory Chanan, Peng Wu, and Soumith Chintala. 2024. PyTorch 2: Faster Machine Learning Through Dynamic Python Bytecode Transformation and Graph Compilation. In *Proceedings of the 29th ACM International Conference on Architectural Support for Programming Languages and Operating Systems, Volume 2 (ASPLOS ’24)*. New York, NY, USA, 929–947. <https://doi.org/10.1145/3620665.3640366>
- [9] Dmitri I Arkhipov, Di Wu, Keqin Li, and Amelia C Regan. 2017. Sorting with gpus: A survey. *arXiv preprint arXiv:1709.02520* (2017).
- [10] Akari Asai, Jacqueline He, Rulin Shao, Weijia Shi, Amanpreet Singh, Joseph Chee Chang, Kyle Lo, Luca Soldaini, Sergey Feldman, Mike D’Arcy, et al. 2024. OpenScholar: Synthesizing Scientific Literature with Retrieval-augmented LMs. *arXiv preprint arXiv:2411.14199* (2024).
- [11] Akari Asai, Zeqiu Wu, Yizhong Wang, Avirup Sil, and Hannaneh Hajishirzi. 2023. Self-RAG: Learning to Retrieve, Generate, and Critique through Self-Reflection. In *The Twelfth International Conference on Learning Representations*.
- [12] Akari Asai, Zeqiu Wu, Yizhong Wang, Avirup Sil, and Hannaneh Hajishirzi. 2024. Original implementation of SELF-RAG: Learning to Retrieve, Generate and Critique through self-reflection. <https://github.com/AkariAsai/self-rag>.
- [13] Akari Asai, Zexuan Zhong, Danqi Chen, Pang Wei Koh, Luke Zettlemoyer, Hannaneh Hajishirzi, and Wen-tau Yih. 2024. Reliable, adaptable, and attributable language models with retrieval. *arXiv preprint arXiv:2403.03187* (2024).
- [14] AWS. [n. d.]. Guidance for Conversational Chatbots Using Retrieval Augmented Generation on AWS. <https://aws.amazon.com/solutions/guidance/conversational-chatbots-using-retrieval-augmented-generation-on-aws/>.
- [15] Emery Berger and Ben Zorn. 2024. AI Software Should be More Like Plain Old Software. <https://www.sigarch.org/ai-software-should-be-more-like-plain-old-software/>.
- [16] Sebastian Borgeaud, Arthur Mensch, Jordan Hoffmann, Trevor Cai, Eliza Rutherford, Katie Millican, George Bm Van Den Driessche, Jean-Baptiste Lespiau, Bogdan Damoc, Aidan Clark, et al. 2022. Improving language models by retrieving from trillions of tokens. In *International conference on machine learning*. PMLR, 2206–2240.
- [17] James Briggs, Gibbs Cullen, and Greg Kogan. [n. d.]. Vector Search in the Wild. <https://www.pinecone.io/learn/series/wild/>.
- [18] Tianhui Cai, Yifan Liu, Zewei Zhou, Haoxuan Ma, Seth Z Zhao, Zhiwen Wu, and Jiaqi Ma. 2024. Driving with Regulation: Interpretable Decision-Making for Autonomous Vehicles with Retrieval-Augmented Reasoning via LLM. *arXiv preprint arXiv:2410.04759* (2024).
- [19] Binoy Chennagat. 2024. Reducing RAG Pipeline Latency for Real-Time Voice Conversations. <https://developer.vonage.com/en/blog/reducing-rag-pipeline-latency-for-real-time-voice-conversations>.
- [20] Qi Chen, Bing Zhao, Haidong Wang, Mingqin Li, Chuanjie Liu, Zengzhong Li, Mao Yang, and Jingdong Wang. 2021. Spann: Highly-efficient billion-scale approximate nearest neighbor search. *arXiv preprint arXiv:2111.08566* (2021).
- [21] Felix Chern, Blake Hechtman, Andy Davis, Ruiqi Guo, David Majner, and Sanjiv Kumar. 2022. TPU-KNN: K nearest neighbor search at peak flop/s. In *Advances in Neural Information Processing Systems*, Vol. 35. 15489–15501.
- [22] Neo Christopher Chung, George Dyer, and Lennart Brocki. 2023. Challenges of large language models for mental health counseling. *arXiv preprint arXiv:2311.13857* (2023).

[23] Databricks. 2024. RAG (Retrieval Augmented Generation) on Databricks. <https://docs.databricks.com/en/generative-ai/retrieval-augmented-generation.html>.

[24] Divyanshu Dixit. 2024. Advanced RAG Series: Generation and Evaluation. <https://div.beehiiv.com/p/advanced-rag-series-generation-evaluation>.

[25] Matthijs Douze, Alexandre Guzhva, Chengqi Deng, Jeff Johnson, Gergely Szilvassy, Pierre-Emmanuel Mazaré, Maria Lomeli, Lucas Hosseini, and Hervé Jégou. 2024. The faiss library. *arXiv preprint arXiv:2401.08281* (2024).

[26] Wenqi Fan, Yujuan Ding, Liangbo Ning, Shijie Wang, Hengyun Li, Dawei Yin, Tat-Seng Chua, and Qing Li. 2024. A Survey on RAG Meeting LLMs: Towards Retrieval-Augmented Large Language Models. In *Knowledge Discovery and Data Mining*. <https://api.semanticscholar.org/CorpusID:269740933>

[27] Luyu Gao, Xueguang Ma, Jimmy Lin, and Jamie Callan. 2023. Precise Zero-Shot Dense Retrieval without Relevance Labels. In *Proceedings of the 61st Annual Meeting of the Association for Computational Linguistics (Volume 1: Long Papers)*. 1762–1777.

[28] Yunfan Gao. 2024. Modular RAG and RAG Flow: Part II. <https://medium.com/@yufan1602/modular-rag-and-rag-flow-part-ii-77b62bf8a5d3>.

[29] Yunfan Gao, Yun Xiong, Xinyu Gao, Kangxiang Jia, Jinliu Pan, Yuxi Bi, Yi Dai, Jiawei Sun, and Haofen Wang. 2023. Retrieval-augmented generation for large language models: A survey. *arXiv preprint arXiv:2312.10997* (2023).

[30] Samira Ghodratnama and Mehrdad Zakershahrak. 2023. Adapting LLMs for Efficient, Personalized Information Retrieval: Methods and Implications. In *International Conference on Service-Oriented Computing*. Springer, 17–26.

[31] Abdussamad GM and Gopala Dhar. 2024. How Apollo 24/7 leverages MedLM with RAG to revolutionize healthcare. <https://cloud.google.com/blog/products/ai-machine-learning/how-apollo-247-leverages-medlm-with-rag-to-revolutionize-healthcare>.

[32] Ruiqi Guo, Philip Sun, Erik Lindgren, Quan Geng, David Simcha, Felix Chern, and Sanjiv Kumar. 2020. Accelerating Large-Scale Inference with Anisotropic Vector Quantization. In *International Conference on Machine Learning*. <https://arxiv.org/abs/1908.10396>

[33] Moritz Hardt and Yu Sun. 2023. Test-time training on nearest neighbors for large language models. *arXiv preprint arXiv:2305.18466* (2023).

[34] Ivan Ilin. 2023. Advanced RAG Techniques: an Illustrated Overview. <https://pub.towardsai.net/advanced-rag-techniques-an-illustrated-overview-04d193d8fec6>.

[35] Gautier Izacard, Mathilde Caron, Lucas Hosseini, Sebastian Riedel, Piotr Bojanowski, Armand Joulin, and Edouard Grave. 2021. Unsupervised dense information retrieval with contrastive learning. *arXiv preprint arXiv:2112.09118* (2021).

[36] Gautier Izacard, Patrick Lewis, Maria Lomeli, Lucas Hosseini, Fabio Petroni, Timo Schick, Jane Dwivedi-Yu, Armand Joulin, Sebastian Riedel, and Edouard Grave. 2023. Atlas: Few-shot learning with retrieval augmented language models. *Journal of Machine Learning Research* 24, 251 (2023), 1–43.

[37] Rolf Jagerman, Honglei Zhuang, Zhen Qin, Xuanhui Wang, and Michael Bendersky. 2023. Query expansion by prompting large language models. *arXiv preprint arXiv:2305.03653* (2023).

[38] Suhas Jayaram Subramanya, Fnu Devvrit, Harsha Vardhan Simhadri, Ravishankar Krishnawamy, and Rohan Kadekodi. 2019. Diskann: Fast accurate billion-point nearest neighbor search on a single node. *Advances in Neural Information Processing Systems* 32 (2019).

[39] Huiqiang Jiang, Qianhui Wu, Xufang Luo, Dongsheng Li, Chin-Yew Lin, Yuqing Yang, and Lili Qiu. 2023. Longllmllingua: Accelerating and enhancing llms in long context scenarios via prompt compression.

[40] Wenqi Jiang, Shigang Li, Yu Zhu, Johannes de Fine Licht, Zhenhao He, Runbin Shi, Cedric Renggli, Shuai Zhang, Theodoros Rekatsinas, Torsten Hoefer, et al. 2023. Co-design hardware and algorithm for vector search. In *Proceedings of the International Conference for High Performance Computing, Networking, Storage and Analysis*. 1–15.

[41] Wenqi Jiang, Suvinay Subramanian, Cat Graves, Gustavo Alonso, Amir Yazdanbakhsh, and Vidushi Dadu. 2025. RAGO: Systematic Performance Optimization for Retrieval-Augmented Generation Serving. *arXiv preprint arXiv:2503.14649* (2025).

[42] Wenqi Jiang, Marco Zeller, Roger Waleffe, Torsten Hoefer, and Gustavo Alonso. 2023. Chameleon: a heterogeneous and disaggregated accelerator system for retrieval-augmented language models. *arXiv preprint arXiv:2310.09949* (2023).

[43] Wenqi Jiang, Shuai Zhang, Boran Han, Jie Wang, Bernie Wang, and Tim Kraska. 2024. Piperag: Fast retrieval-augmented generation via algorithm-system co-design. *arXiv preprint arXiv:2403.05676* (2024).

[44] Zhengbao Jiang, Frank F. Xu, Luyu Gao, Zhiqing Sun, Qian Liu, Jane Dwivedi-Yu, Yiming Yang, Jamie Callan, and Graham Neubig. 2023. Active Retrieval Augmented Generation. (2023). *arXiv:2305.06983* [cs.CL]

[45] Chao Jin, Zili Zhang, Xuanlin Jiang, Fangyue Liu, Xin Liu, Xuanzhe Liu, and Xin Jin. 2024. RAGCache: Efficient Knowledge Caching for Retrieval-Augmented Generation. *arXiv preprint arXiv:2404.12457* (2024).

[46] Jiajie Jin, Yutao Zhu, Xinyu Yang, Chenghao Zhang, and Zhicheng Dou. 2024. FlashRAG: A Modular Toolkit for Efficient Retrieval-Augmented Generation Research. *arXiv preprint arXiv:2405.13576* (2024).

[47] Jeff Johnson, Matthijs Douze, and Hervé Jégou. 2019. Billion-scale similarity search with GPUs. *IEEE Transactions on Big Data* 7, 3 (2019), 535–547.

[48] Mandar Joshi, Eunsol Choi, Daniel S Weld, and Luke Zettlemoyer. 2017. TriviaQA: A Large Scale Distantly Supervised Challenge Dataset for Reading Comprehension. In *Proceedings of the 55th Annual Meeting of the Association for Computational Linguistics (Volume 1: Long Papers)*. 1601–1611.

[49] Vladimir Karpukhin, Barlas Ouz, Sewon Min, Patrick Lewis, Ledell Wu, Sergey Edunov, Danqi Chen, and Wen-tau Yih. 2020. Dense Passage Retrieval for Open-Domain Question Answering. <https://www.aclweb.org/anthology/2020.emnlp-main.550>. In *Proceedings of the 2020 Conference on Empirical Methods in Natural Language Processing (EMNLP)*.

[50] Saim Khan, Somesh Singh, Harsha Vardhan Simhadri, Jyothi Vedurada, et al. 2024. BANG: Billion-Scale Approximate Nearest Neighbor Search using a Single GPU. *arXiv preprint arXiv:2401.11324* (2024).

[51] Urvashi Khandelwal, Omer Levy, Dan Jurafsky, Luke Zettlemoyer, and Mike Lewis. 2019. Generalization through Memorization: Nearest Neighbor Language Models. In *International Conference on Learning Representations*.

[52] Jaehyung Kim, Jaehyun Nam, Sangwoo Mo, Jongjin Park, Sang-Woo Lee, Minjoon Seo, Jung-Woo Ha, and Jinwoo Shin. 2023. SuRe: Improving Open-domain Question Answering of LLMs via Summarized Retrieval. In *The Twelfth International Conference on Learning Representations*.

[53] Sehoon Kim, Suhong Moon, Ryan Tabrizi, Nicholas Lee, Michael W Mahoney, Kurt Keutzer, and Amir Gholami. 2023. An LLM compiler for parallel function calling. *arXiv preprint arXiv:2312.04511* (2023).

[54] Eyal Klang, Idit Tessler, Donald U Apakama, Ethan Abbott, Benjamin S Glicksberg, Monique Arnold, Akini Moses, Ankit Sakhija, Ali Soroush, Alexander W Charney, et al. 2024. Assessing Retrieval-Augmented Large Language Model Performance in Emergency Department ICD-10-CM Coding Compared to Human Coders. *medRxiv* (2024).

[55] Tom Kwiatkowski, Jennimaria Palomaki, Olivia Redfield, Michael Collins, Ankur Parikh, Chris Alberti, Danielle Epstein, Illia Polosukhin, Jacob Devlin, Kenton Lee, et al. 2019. Natural questions: a benchmark for question answering research. *Transactions of the Association for Computational Linguistics* 7 (2019), 453–466.

[56] Woosuk Kwon, Zhuohan Li, Siyuan Zhuang, Ying Sheng, Lianmin Zheng, Cody Hao Yu, Joseph E. Gonzalez, Hao Zhang, and Ion Stoica. 2023. Efficient Memory Management for Large Language Model Serving with PagedAttention. In *Proceedings of the ACM SIGOPS 29th Symposium on Operating Systems Principles*.

[57] Maximilian Lam, Jeff Johnson, Wenjie Xiong, Kiwan Maeng, Udit Gupta, Yang Li, Liangzhen Lai, Ilias Leontiadis, Minsoo Rhu, Hsien-Hsin S. Lee, Vijay Janapa Reddi, Gu-Yeon Wei, David Brooks, and G. Edward Suh. 2023. GPU-based Private Information Retrieval for On-Device Machine Learning Inference. arXiv:2301.10904 [cs.CR] <https://arxiv.org/abs/2301.10904>

[58] Patrick Lewis, Ethan Perez, Aleksandra Piktus, Fabio Petroni, Vladimir Karpukhin, Naman Goyal, Heinrich Küttler, Mike Lewis, Wen-tau Yih, Tim Rocktäschel, et al. 2020. Retrieval-augmented generation for knowledge-intensive nlp tasks. *Advances in Neural Information Processing Systems* 33 (2020), 9459–9474.

[59] Jerry Liu. 2022. *LlamaIndex*. doi:10.5281/zenodo.1234

[60] Zihan Liu, Wentao Ni, Jingwen Leng, Yu Feng, Cong Guo, Quan Chen, Chao Li, Minyi Guo, and Yuhao Zhu. 2023. JUNO: Optimizing High-Dimensional Approximate Nearest Neighbour Search with Sparsity-Aware Algorithm and Ray-Tracing Core Mapping. *arXiv preprint arXiv:2312.01712* (2023).

[61] Songshuo Lu, Hua Wang, Yutian Rong, Zhi Chen, and Yaohua Tang. 2024. TurboRAG: Accelerating Retrieval-Augmented Generation with Precomputed KV Caches for Chunked Text. *arXiv preprint arXiv:2410.07590* (2024).

[62] Xinbei Ma, Yeyun Gong, Pengcheng He, Nan Duan, et al. 2023. Query Rewriting in Retrieval-Augmented Large Language Models. In *The 2023 Conference on Empirical Methods in Natural Language Processing*.

[63] Melissa Malec. 2024. RAG in Financial Services: Use-Cases, Impact, & Solutions. <https://hatchworks.com/blog/gen-ai/rag-for-financial-services/>.

[64] Alex Troy Mallen, Akari Asai, Victor Zhong, Rajarshi Das, Daniel Khashabi, and Hannaneh Hajishirzi. 2023. When Not to Trust Language Models: Investigating Effectiveness of Parametric and Non-Parametric Memories. In *The 61st Annual Meeting Of The Association For Computational Linguistics*.

[65] Sewon Min, Suchin Gururangan, Eric Wallace, Weijia Shi, Hannaneh Hajishirzi, Noah A Smith, and Luke Zettlemoyer. 2023. SILO Language Models: Isolating Legal Risk In a Nonparametric Datastore. In *The Twelfth International Conference on Learning Representations*.

[66] MyScale. 2024. 4 Key Benefits of RAG Algorithmic Trading in Financial Markets. <https://myscale.com/blog/benefits-rag-algorithmic-trading-financial-markets/>.

[67] Mohammad Norouzi and David J Fleet. 2013. Cartesian k-means. In *Proceedings of the IEEE Conference on computer Vision and Pattern Recognition*. 3017–3024.

[68] NVIDIA. 2024. GeForce RTX 4090. <https://www.nvidia.com/en-us/geforce/graphics-cards/40-series/rtx-4090/>.

[69] NVIDIA. 2024. NVIDIA H100 Tensor Core GPU. <https://resources.nvidia.com/en-us-tensor-core/nvidia-tensor-core-gpu-datasheet>.

[70] OpenAI. [n. d.]. GPT-3.5 Turbo. <https://platform.openai.com/docs/models/gpt-3-5-turbo>.

[71] Pathway. 2024. Adaptive RAG: How we cut LLM costs without sacrificing accuracy. <https://pathway.com/developers/showcases/adaptive-rag>.

[72] Wenjun Peng, Guiyang Li, Yue Jiang, Zilong Wang, Dan Ou, Xiaoyi Zeng, Tongxu, and Enhong Chen. 2023. Large Language Model based Long-tail Query Rewriting in Taobao Search. *Companion Proceedings of the ACM on Web Conference 2024* (2023). <https://api.semanticscholar.org/CorpusID:265042961>

[73] Wenjun Peng, Guiyang Li, Yue Jiang, Zilong Wang, Dan Ou, Xiaoyi Zeng, Derong Xu, Tong Xu, and Enhong Chen. 2024. Large Language Model based Long-tail Query Rewriting in Taobao Search. In *Companion Proceedings of the ACM on Web Conference 2024*.

[74] Ofir Press, Muru Zhang, Sewon Min, Ludwig Schmidt, Noah A Smith, and Mike Lewis. 2023. Measuring and Narrowing the Compositionality Gap in Language Models. In *Findings of the Association for Computational Linguistics: EMNLP 2023*. 5687–5711.

[75] Derrick Quinn, Mohammad Nouri, Neel Patel, John Salihu, Alireza Salemi, Sukhan Lee, Hamed Zamani, and Mohammad Alian. 2025. Accelerating Retrieval-Augmented Generation. In *Proceedings of the 30th ACM International Conference on Architectural Support for Programming Languages and Operating Systems, Volume 1* (Rotterdam, Netherlands) (ASPLOS '25). Association for Computing Machinery, New York, NY, USA, 15–32. doi:10.1145/3669940.3707264

[76] Ori Ram, Yoav Levine, Itay Dalmedigos, Dor Muhlgay, Amnon Shashua, Kevin Leyton-Brown, and Yoav Shoham. 2023. In-Context Retrieval-Augmented Language Models. *Transactions of the Association for Computational Linguistics* 11 (2023), 1316–1331.

[77] Rapidsai. 2022. Rapidsai/raft: RAFT contains fundamental widely-used algorithms and primitives for data science, Graph and machine learning. <https://github.com/rapidsai/raft>.

[78] Korakit Seemakupt, Sihang Liu, and Samira Khan. 2024. EdgeRAG: Online-Indexed RAG for Edge Devices. arXiv:2412.21023 [cs.LG] <https://arxiv.org/abs/2412.21023>

[79] Rulin Shao, Jacqueline He, Akari Asai, Weijia Shi, Tim Dettmers, Sewon Min, Luke Zettlemoyer, and Pang Wei Koh. [n. d.]. Scaling Retrieval-Based Language Models with a Trillion-Token Datastore. In *The Thirty-eighth Annual Conference on Neural Information Processing Systems*.

[80] Zhihong Shao, Yeyun Gong, Yelong Shen, Minlie Huang, Nan Duan, and Weizhu Chen. 2023. Enhancing Retrieval-Augmented Large Language Models with Iterative Retrieval-Generation Synergy. In *Findings of the Association for Computational Linguistics: EMNLP 2023*. 9248–9274.

[81] Josef Sivic and Andrew Zisserman. 2003. Video Google: A Text Retrieval Approach to Object Matching in Videos.. In *ICCV*. IEEE Computer Society, 1470–1477.

[82] David Stewart and Jamie Linsdell. 2024. Say Hello to Precision: How Rerankers and Embeddings Boost Search. <https://cohere.com/blog/say-hello-to-precision-how-rerankers-and-embeddings-boost-search>.

[83] Hugo Touvron, Louis Martin, Kevin Stone, Peter Albert, Amjad Almahairi, Yasmine Babaei, Nikolay Bashlykov, Soumya Batra, Prajwal Bhargava, Shruti Bhosale, et al. 2023. Llama 2: Open foundation and fine-tuned chat models. *arXiv preprint arXiv:2307.09288* (2023).

[84] Kuan Tung. 2024. Enhancing User Experience by Overcoming Latency in the ION IQ Chatbot. <https://www.ontinue.com/resource/enhancing-user-experience-by-overcoming-latency-in-the-ion-iq-chatbot/>.

[85] Niithiyin Vijeaswaran, AJ Dhimine, Armando Diaz, Sebastian Bustillo, Farooq Sabir, and Marco Punio. 2024. Advanced RAG patterns on Amazon SageMaker. <https://aws.amazon.com/blogs/machine-learning/advanced-rag-patterns-on-amazon-sagemaker/>.

[86] Lei Wang, Chen Ma, Xueyang Feng, Zeyu Zhang, Hao Yang, Jingsen Zhang, Zhiyuan Chen, Jiakai Tang, Xu Chen, Yankai Lin, et al. 2024. A survey on large language model based autonomous agents. *Frontiers of Computer Science* 18, 6 (2024), 186345.

[87] Zilong Wang, Zifeng Wang, Long Le, Huaixiu Steven Zheng, Swaroop Mishra, Vincent Perot, Yuwei Zhang, Anush Mattapalli, Ankur Taly, Jingbo Shang, et al. 2024. Speculative rag: Enhancing retrieval augmented generation through drafting. *arXiv preprint arXiv:2407.08223*

(2024).

[88] Zijie J. Wang and Duen Horng Chau. 2024. MeMemo: On-device Retrieval Augmentation for Private and Personalized Text Generation. In *Proceedings of the 47th International ACM SIGIR Conference on Research and Development in Information Retrieval* (Washington DC, USA) (SIGIR '24). Association for Computing Machinery, New York, NY, USA, 2765–2770. doi:10.1145/3626772.3657662

[89] Khye Wei. 2024. Advanced RAG with Azure AI Search and LlamaIndex. <https://techcommunity.microsoft.com/t5/ai-azure-ai-services-blog/advanced-rag-with-azure-ai-search-and-llamaindex/ba-p/4115007>.

[90] Lukas Wutschitz, Boris Köpf, Andrew Paverd, Saravan Rajmohan, Ahmed Salem, Shruti Tople, Santiago Zanella-Béguelin, Menglin Xia, and Victor Rühle. 2023. Rethinking Privacy in Machine Learning Pipelines from an Information Flow Control Perspective. arXiv:2311.15792 [cs.LG] <https://arxiv.org/abs/2311.15792>

[91] Zhiqiang Xie, Hao Kang, Ying Sheng, Tushar Krishna, Kayvon Fatahalian, and Christos Kozyrakis. 2024. AI Metropolis: Scaling Large Language Model-based Multi-Agent Simulation with Out-of-order Execution. *arXiv preprint arXiv:2411.03519* (2024).

[92] Zhilin Yang, Peng Qi, Saizheng Zhang, Yoshua Bengio, William W. Cohen, Ruslan Salakhutdinov, and Christopher D. Manning. 2018. HotpotQA: A Dataset for Diverse, Explainable Multi-hop Question Answering. In *Conference on Empirical Methods in Natural Language Processing (EMNLP)*.

[93] Jiayi Yao, Hanchen Li, Yuhang Liu, Siddhant Ray, Yihua Cheng, Qizheng Zhang, Kuntai Du, Shan Lu, and Junchen Jiang. 2024. CacheBlend: Fast Large Language Model Serving for RAG with Cached Knowledge Fusion. arXiv:2405.16444 [cs.LG] <https://arxiv.org/abs/2405.16444>

[94] Fanghua Ye, Meng Fang, Shenghui Li, and Emine Yilmaz. 2023. Enhancing Conversational Search: Large Language Model-Aided Informative Query Rewriting. In *The 2023 Conference on Empirical Methods in Natural Language Processing*.

[95] Jianhao Yuan, Shuyang Sun, Daniel Omeiza, Bo Zhao, Paul Newman, Lars Kunze, and Matthew Gadd. 2024. Rag-driver: Generalisable driving explanations with retrieval-augmented in-context learning in multi-modal large language model. *arXiv preprint arXiv:2402.10828* (2024).

[96] Matei Zaharia, Omar Khatab, Lingjiao Chen, Jared Quincy Davis, Heather Miller, Chris Potts, James Zou, Michael Carbin, Jonathan Frankle, Naveen Rao, and Ali Ghodsi. 2024. The Shift from Models to Compound AI Systems. <https://bair.berkeley.edu/blog/2024/02/18/compound-ai-systems/>.

[97] Chaoliang Zeng, Laylong Luo, Qingsong Ning, Yaodong Han, Yuhang Jiang, Ding Tang, Zilong Wang, Kai Chen, and Chuanxiong Guo. 2022. FAERY: An FPGA-accelerated Embedding-based Retrieval System. In *16th USENIX Symposium on Operating Systems Design and Implementation (OSDI 22)*. 841–856.

[98] Zili Zhang, Fangyu Liu, Gang Huang, Xuanzhe Liu, and Xin Jin. 2024. Fast Vector Query Processing for Large Datasets Beyond GPU Memory with Reordered Pipelining. In *21st USENIX Symposium on Networked Systems Design and Implementation (NSDI 24)*. 23–40.

[99] Zhihao Zhang, Alan Zhu, Lijie Yang, Yihua Xu, Lanting Li, Phitchaya Mangpo Phothilimthana, and Zhihao Jia. 2024. Accelerating retrieval-augmented language model serving with speculation. *arXiv preprint arXiv:2401.14021* (2024).

[100] Huaixiu Steven Zheng, Swaroop Mishra, Xinyun Chen, Heng-Tze Cheng, Ed H Chi, Quoc V Le, and Denny Zhou. 2023. Take a step back: Evoking reasoning via abstraction in large language models. *arXiv preprint arXiv:2310.06117* (2023).

[101] Lianmin Zheng, Liangsheng Yin, Zhiqiang Xie, Chuyue Sun, Jeff Huang, Cody Hao Yu, Shiyi Cao, Christos Kozyrakis, Ion Stoica, Joseph E. Gonzalez, Clark Barrett, and Ying Sheng. 2024. SGLang: Efficient Execution of Structured Language Model Programs. arXiv:2312.07104 [cs.AI] <https://arxiv.org/abs/2312.07104>

[102] Denny Zhou, Nathanael Schärli, Le Hou, Jason Wei, Nathan Scales, Xuezhi Wang, Dale Schuurmans, Claire Cui, Olivier Bousquet, Quoc V Le, et al. 2022. Least-to-Most Prompting Enables Complex Reasoning in Large Language Models. In *The Eleventh International Conference on Learning Representations*.

[103] Yuhao Zhu. 2022. RTNN: Accelerating Neighbor Search Using Hardware Ray Tracing. In *Proceedings of the 27th ACM SIGPLAN Symposium on Principles and Practice of Parallel Programming (PPoPP '22)*. 76–89. doi:10.1145/3503221.3508409

[104] Shengyao Zhuang, Bing Liu, Bevan Koopman, and Guido Zuccon. 2023. Open-source Large Language Models are Strong Zero-shot Query Likelihood Models for Document Ranking. In *Findings of the Association for Computational Linguistics: EMNLP 2023*. 8807–8817.

[105] Zilliz. 2020. How to Select Index Parameters for IVF Index. <https://zilliz.com/blog/select-index-parameters-ivf-index>.